ARTICLE

Synthesis and Coordination Behaviour of Aluminate-based Quinolyl Ligands

Received 00th January 20xx,
Accepted 00th January 20xx

DOI: 10.1039/x0xx00000x

Jessica E. Waters,[a] Schirin Hanf,[b] Marina Rincón-Nocito,[a] Andrew D. Bond,[a] Raul García-Rodríguez,[c] Dominic S. Wright,[a,*] Annie L. Colebatch[d,*]

The effects of moving the donor N-atom from the 2-position in lithium (2-pyridyl)- and (2-quinolyl)aluminates to the more remote position in (8-quinolyl)aluminates have been investigated by solid-state structural and DFT computational studies of the new complexes [{EtAl(2-qy)$_3$}Li(μ-X)Li(THF)$_3$] (X = Cl/Br 62:38) [(**1**)Li(μ-X)Li(THF)$_3$], [{(EtAl(2-qy)$_3$)Li}$_2$(μ-Br)]$^-$Li(THF)$_4^+$ [{**1**Li}$_2$(μ-Br)]$^-$Li(THF)$_4^+$, [{EtAl(2-Me-8-qy)$_3$}Li] [(**2**)Li], [{Me$_2$Al(2-Me-8-qy)$_2$}Li(THF)] [(**3a**)Li(THF)], [{Me$_2$Al(6-Me-2-py)$_2$}Li(THF)$_2$] [(**4**)Li(THF)$_2$] and [{{EtAl(2-Me-8-qy)$_2$}$_2$O}(Li$_2$THF)] (**5**). Increasing the remoteness of the donor N-atom from the bridgehead results in large differences in the coordination of the Li$^+$ cations by the (8-quinolyl)aluminate anions compared to 2-quinolyl or 2-pyridyl counterparts. The results are of potential interest in understanding how the coordination sites of ligands of this type can be tuned for the coordination requirements of specific metal centres.

Introduction

The development of tripodal, facially-coordinating ligands has been an important and on-going challenge over the past three decades. Such ligands have extensive applications in modern coordination, organometallic and biomimetic chemistry, as well as in catalysis.[1–5] Tris(pyrazolyl)borate (Tp$^-$) ligands, first synthesised by Trofimenko and co-workers (Fig. 1a),[6] are one of the most versatile families of tripodal ligands, in part arising from the ability to tune their steric and electronic properties by introducing substituents in their pyrazolyl moieties.[7–9] Although they have been studied to a considerably lesser extent than their tris(pyrazolyl)borate relatives, tris(2-pyridyl) ligands have emerged as another important class. The majority of studies in the past four decades have focused on ligands of the type E(2-py)$_3$ containing lighter, non-metallic bridgehead atoms (py = pyridyl, E = CR, COR', CH, N, P, P=O, *etc*; Fig. 1b).[10] These ligands have found a variety of applications similar to their tris(pyrazolyl) counterparts.[11] Until fairly recently, however, few examples have included bridgehead atoms beyond Period 3 of the periodic table.[12]

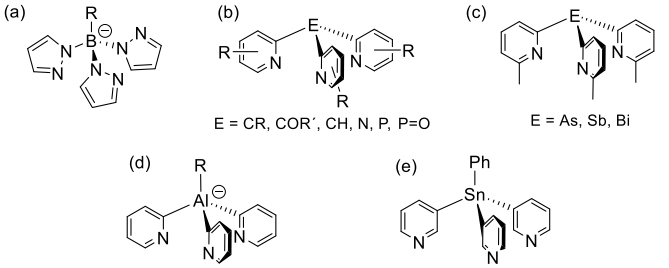

Figure 1 Notable examples of C_3-symmetric tripodal ligands featuring a range of bridgeheads and donor groups; (a) tris(pyrazolyl)borate anion, (b) "classical" neutral tris(2-pyridyl) ligands, (c) tris(2-pyridyl) ligands, E(6-Me-2-py)$_3$, containing heaver Group 15 elements, (d) tris(2-pyridyl)aluminate anion, (e) example of a tris(3-pyridyl) ligand, PhSn(3-py)$_3$.

The incorporation of heavier, more metallic bridgehead atoms into tris(2-pyridyl) ligands provides a means of changing their donor properties systematically by descending a particular p-block group. This has been demonstrated by a recent study of the neutral Group 15 tris(2-pyridyl) ligands E(6-Me-2-py)$_3$, (E = As, Sb, Bi, Fig. 1c) in which it was shown that the increase in the Lewis acidity of the bridgehead can be used to modulate both their coordination behaviour and the catalytic activity of their complexes.[13] In addition, by changing the element or oxidation state of the bridgehead new anionic variants can be accessed which are directly analogous to tris(pyrazolyl)borates. Tris(2-pyridyl)aluminates, [RAl(2-py')$_3$]$^-$ (R = alkyl, py' = substituted pyridyl, e.g., Fig. 1d) are a particularly interesting class of these anionic ligands, which have found applications in the formation of lanthanoid(II) sandwich complexes,[14] in the iron-catalysed epoxidation of styrene[11] and as chiral discrimination reagents.[15]

[a] *Yusuf Hamied Department of Chemistry, University of Cambridge, Lensfield Road, Cambridge CB2 1EW; E-mail: dsw1000@cam.ac.uk.*
[b] *Karlsruhe Institut für Technologie (KIT), 76131 Karlsruhe, Baden-Württemberg Germany*
[c] *GIR MIOMeT-IU Cinquima-Química, Inorgunica Facultad de Ciencias, Universidad de Valladolid, Campus Miguel Delibes, 47011 Valladolid*
[d] *Research School of Chemistry, The Australian National University, Canberra ACT 2601, Australia; E-mail: annie.colebatch@anu.edu.au*

† Electronic Supplementary Information (ESI) available: details of synthesis, spectroscopy, calculations and X-ray crystallography. CCDC 2096424-2096428, 2097862. See DOI: 10.1039/x0xx00000x.

Closely related anionic tris(2-pyridyl)borates have also been employed recently in a range of materials applications.[16]

Changing the position of the donor N-atoms within the pyridyl ring units from the 2- to 3-position significantly alters the coordination characteristics, allowing the coordination of more than one metal centre. Studies of the Group 14 ligands MeSi(3-py)$_3$[17] and PhSn(3-py)$_3$ (Fig. 1e)[18] have shown that these can form a range of extended and molecular supramolecular arrangements with various metal ions. So far, however, the functionalisation of tris(pyridyl) ligands with polyaromatic N-donor groups has been largely ignored as a means of modifying the coordination site, the only example of this type containing a heavier element bridgehead being MeSi(3-qy)$_3$ (qy = quinolyl).[17a] However, an earlier study showed that sequential replacement of 2-pyridyl groups with 2-quinolyl substituents in the HC(2-py)$_3$ ligand can lead to large changes in the geometries of coordinated metal centres.[19] The quinolyl substituent is a particularly interesting candidate for ligand modification since the position of the donor N-atom relative to the bridgehead atom can be changed readily, making the coordinated metal centre closer (i.e., 2-qy) or further away (i.e., 8-qy) from the bridgehead (Figure 2).

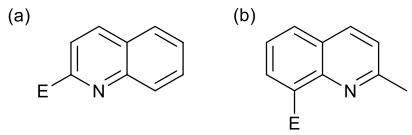

Figure 2 (a) 2-quinolyl (2-qy), and (b) 2-Me-8-quinolyl (2-Me-8-qy) variants presented in this study.

In this study we investigate the synthesis and coordination properties of a series of tris(3-quinolyl) aluminate ligands containing 2-qy and 8-qy substituents.

Results and Discussion

With the previous background in mind, we set out to obtain a range of bis- and tris-quinolyl ligands containing main group bridgehead atoms. The new compounds synthesised in the current study are shown in Figure 3, which also shows the numbering scheme used throughout the discussion and experimental sections.

Our studies started by exploring the synthesis of the aluminate anion [EtAl(2-qy)$_3$]$^-$ (**1**), in which the N-donor functionality is in close proximity to the Al^{III} bridgehead, providing a similar environment for metal coordination to the previously explored aluminates [RAl(2-py)$_3$]$^-$. However, lithiation of 2-bromo-quinoline with ^{n}BuLi at –78 °C in THF followed by in situ reaction of the intermediate 2-lithio-quinoline with EtAlCl$_2$ (3:1 equiv.) only afforded a small crop of crystalline material, which contained a mixture of the ion-paired complex [(**1**)Li(μ-X)Li(THF)$_3$] (X = Cl/Br in a ratio of 62:38, respectively) and ion-separated complex [{**1**Li}$_2$(μ-Br)]$^-$Li(THF)$_4^+$ (as shown by single-crystal X-ray diffraction studies, Scheme 1). The reason for the low yield appears to be the instability of the anion **1**, presumably to reductive elimination to form 2,2′-biquinoline, which was detected in the ^{1}H NMR spectroscopic and HR-MS studies of the crude reaction mixture (see ESI). Similar reductive elimination processes have been observed with tris(2-pyridyl) systems involving other main group element bridgeheads.[12,13]

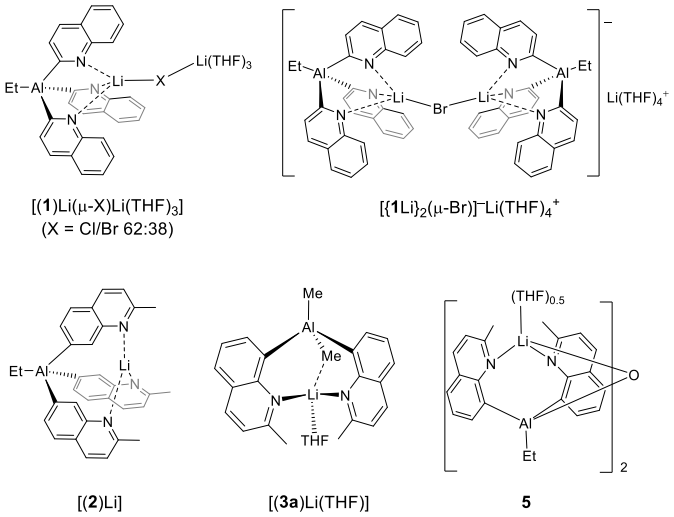

Figure 3 Bis- and tris(quinolyl)-based main group ligands and complexes explored in the current study: [{EtAl(2-qy)$_3$}Li(μ-X)Li(THF)$_3$] (X = Cl/Br 62:38) [(**1**)Li(μ-X)Li(THF)$_3$], [{(EtAl(2-qy)$_3$)Li}$_2$(μ-Br)]$^-$Li(THF)$_4^+$ [{**1**Li}$_2$(μ-Br)]$^-$Li(THF)$_4^+$, [{EtAl(2-Me-8-qy)$_3$}Li] [(**2**)Li], [{Me$_2$Al(2-Me-8-qy)$_2$}Li(THF)] [(**3a**)Li(THF)], and [{{EtAl(2-Me-8-qy)$_2$}$_2$O}(Li$_2$THF)] (**5**).

The solid-state structures of [(**1**)Li(μ-X)Li(THF)$_3$] and of the [{**1**Li}$_2$(μ-Br)]$^-$ anion are shown in Figure 4. Both complexes have conceptually similar arrangements, in which one of the Li$^+$ cations is coordinated by the three N-atoms of the aluminate **1**, with the pseudo-tetrahedral geometry being completed by a halide (Cl$^-$ or Br$^-$) anion. The halide ions bridge the two Li$^+$ cations (with a Li(THF)$_3^+$ or (**1**)Li fragment). The structures are similar to those observed previously for the tris(2-pyridyl)aluminate complexes [MeAl(3-Me-2-py)$_3$Li(μ-Br)Li(THF)$_3$][20] and [{MeAl(2-py)$_3$}$_2$Li(μ-Cl)]$^-$.[21] The similarity of the new 2-qy complexes to these previous examples is perhaps unsurprising, bearing in mind the similar position of the N-donor atoms, and indicates that the presence of the fused-benzene substituent has little effect on the coordination environment compared to the parent (2-pyridyl)aluminates.

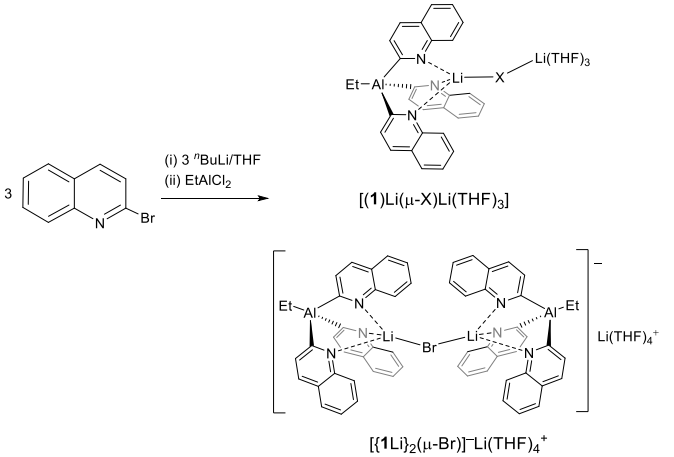

Scheme 1 Synthesis of [(**1**)Li(μ-X)Li(THF)$_3$] (X = Cl/Br 62:38) and ion-separated complex [{**1**Li}$_2$(μ-Br)]$^-$Li(THF)$_4^+$.

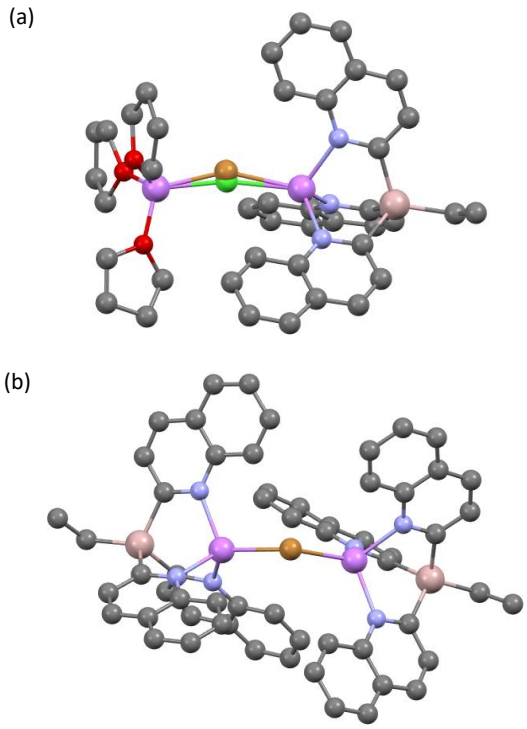

Figure 4 (a) Structure of [(**1**)Li(μ-X)Li(THF)$_3$] (X = Cl/Br 62:38) and (b) the anion [{**1**Li}$_2$(μ-Br)]$^-$. H-atoms and lattice solvation have been omitted for clarity. Selected bond lengths (Å) and angles (°): [(**1**)Li(μ-X)Li(THF)$_3$]: C_{Et}-Al 1.987(7), C_{qy}-Al range 2.007(6)-2.021(6), N-Li range 2.164(10)-2.191(10), Al•••Li 3.060(9), Li-O range 1.880(12)-1.902(11), Li-X range 2.32(2)-2.511(15), C_{qy}-Al-C_{qy} range 104.4(2)-106.1(2), N-Li-N range 100.9(4)-104.8(4), Li-Cl-Li 164.6(9), Li-Br-Li 153.2(8). [{**1**Li}$_2$(μ-Br)]$^-$: C_{Et}-Al range 1.978(7)-1.980(7), C_{qy}-Al range 2.009(7)-2.022(7), N-Li range 2.145(11)-2.198(12), Al•••Li range 3.054(11)-3.058(10), Li-Br range 2.558(11)-2.568(10), C_{qy}-Al-C_{qy} range 101.9(3)-107.6(3), N-Li-N range 97.2(4)-108.8(5), N-Li-Br range 111.0(4)-118.8(5), Li-Br-Li range 126.0(5)-129.0(5). Colour code: C (grey), Al (pink), N (blue), Li (magenta), Cl (green), Br (brown), O (red).

In light of our initial work on the (2-quinolyl)aluminates, we decided to direct our investigation to aluminates incorporating 2-methyl-8-quinolyl substituents. In previous work on tris(2-pyridyl) ligand systems we had shown that the presence of a Me-substituent adjacent to the donor N-atom increases the stability by supressing the elimination of bipyridines. At the same time, it was reasoned that the greater separation of the N-donor atoms from the bridgehead would result in a significantly different coordination environment. Lithium-halogen exchange of 8-bromo-2-methylquinoline with ^{n}BuLi was accomplished at –78 °C in THF, followed by (3:1) reaction with $EtAlCl_2$ (Scheme 2). Crystals of the new complex [{EtAl(2-Me-8-qy)$_3$}Li] [(**2**)Li] were obtained in 42% yield after workup. The room-temperature ^{1}H NMR spectrum in D_8-THF shows the expected 1:3 ratio of the Et and 2-Me-8-qy groups. The single-crystal X-ray structure of (**2**)Li is that of a monomeric arrangement in which the Li$^+$ cation has a trigonal planar geometry [N-Li-N range 118.97(3)-120.45(3)°]. This appears to result from a combination of the geometric disposition of the quinolyl N-donor atoms and the steric shielding of the Li-centre (which is therefore not able to attain a tetrahedral geometry by the coordination of a THF molecule). It can be noted in this regard that (albeit weak) coordination of the Li$^+$ cation by a THF ligand *does* occur in the analogous lithium tris(2-pyridyl)aluminate complex [{EtAl(6-Me-2-py)$_3$}Li(THF)],[22] also containing Me-groups adjacent to the N-donor atoms (i.e., in a similar position to those present in (**2**)Li). The trigonal planar geometry observed in (**2**)Li is in marked contrast to the three-coordinate, pyramidal geometry of the Li$^+$ cation found in the unsolvated complex [{EtAl(6-Me-2-py)$_3$}Li],[23] resulting from the loss of THF from [{EtAl(6-Me-2-py)$_3$}Li(THF)].

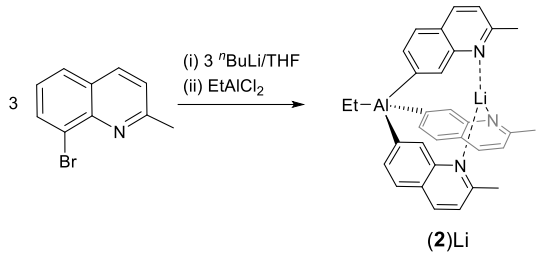

Scheme 2 Synthesis of (**2**)Li.

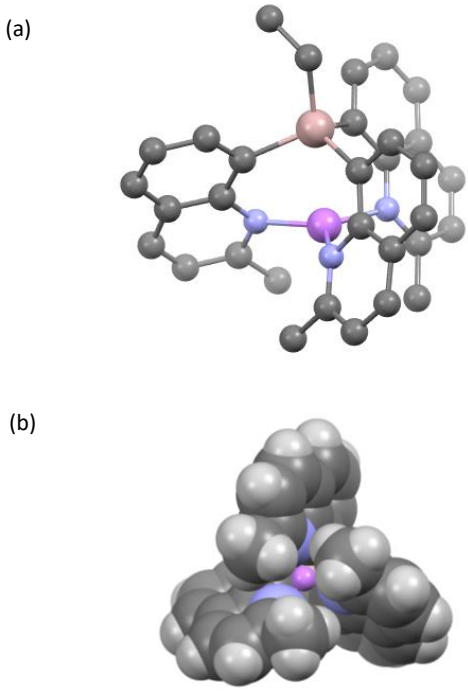

Figure 5 (a) Structure of (**2**)Li. H-atoms and THF lattice solvent have been omitted for clarity. Selected bond lengths (Å) and angles (°): C_{Et}-Al 2.000(3), C_{qy}-Al range 2.043(3)-2.052(3), N-Li range 1.952(5)-1.971(5), Al•••Li 2.736(5), C_{qy}-Al-C_{qy} range 109.27(11)-113.97(12), N-Li-N range 118.9(2)-120.6(3). (b) View of the molecules down the approximate Al•••Li C_3-axis of the molecules, showing the sterically-shielded Li$^+$ cation and the distorted arrangement of the three 2-Me-8-qy substituents. Colour code: C (grey), Al (pink), N (blue), Li (magenta).

Unexpectedly, despite the apparently greater remoteness of the coordinated Li$^+$ cation in (**2**)Li from the bridgehead Al centre compared to 2-pyridyl aluminates, the Al•••Li separation (2.736(5) Å) is significantly shorter than that seen in tris(2-pyridyl)aluminate complexes (e.g., mean 2.84 Å in [{EtAl(6-Me-2-py)$_3$}Li][23]). The accommodation of the trigonal planar Li$^+$ cation within the coordination site of the aluminate anion **2** results in noticeable misalignment of the sp^2 lone pairs of the N-atoms, with the planes of the quinolyl groups being tilted by ca.

30° with respect to the N-Li bond axes (Figure 5b). This suggests that there is significant strain in this arrangement.

A similar synthetic procedure involving lithiation of 8-bromo-2-methylquinoline in THF and in situ reaction of the intermediate lithio-quinoline in a 2:1 stoichiometric ratio with Me_2AlCl gave the bis(2-methyl-8-quinolyl)aluminate complex [{Me_2Al(2-Me-8-qy)$_2$}Li(THF)] [(**3a**)Li(THF)] (Scheme 3). This was isolated in 50% yield after crystallisation from toluene. The solid-state structure was determined by single-crystal X-ray analysis. The structure is that of a monomer in which the [Me_2Al(2-Me-8-qy)$_2$]$^-$ anion (**3a**) coordinates the Li^+ cation via the two qy-N atoms (Li-N range 2.046(5)-2.075(5) Å), with the Al•••Li contact (2.808(4) Å) being slightly longer than that seen in (**2**)Li (Figure 6). Further Li^+ coordination by a THF molecule, and the presence of an additional Al–Me•••Li interaction with one of the Me groups of the Al bridgehead, results in a distorted trigonal pyramidal geometry at the Li centre (in which the N and O atoms are approximately coplanar). The most significant Me•••Li interaction in the complex (C•••Li 2.449(5) Å; H•••Li 1.84 Å) compares to mean C•••Li and H•••Li distances of 2.285 and 2.07 Å, respectively, found in previously reported lithium aluminates containing similar interactions.[24,25] In addition, there are two longer-range C–H•••Li interactions with the 2-Me groups of the quinolyl ligands (2.61 Å). It is worthwhile noting that the type of bridgehead alkyl•••Li interaction found in [(**3a**)Li(THF)] has not been observed in the few previously reported bis(2-pyridyl) Group 13 complexes of Ga and In[26] – [(**3a**)Li(THF)] being the first bis-aluminate of this class.

Although the two Me–Al groups are inequivalent in the solid-state structure, the room temperature ^{1}H NMR spectrum shows only one Me resonance (at δ –0.34 ppm in D_8-THF), suggesting fluxionality. However, variable temperature ^{1}H NMR data revealed no splitting of this peak, even at substantially low temperatures (ca. 238 K), suggesting that the activation energy for this process is very low. Confirmation of the persistence of the C–(H)•••Li interactions in solution and the maintenance of its molecular structure is seen in the ^{1}H-^{7}Li HOESY NMR spectrum, which shows two (albeit weak) correlations to the Li^+ cation – one to the Al-CH_3 peak at δ −0.34 ppm and another to the 2-Me substituents of the quinolyl group at δ 2.58 ppm (see ESI).

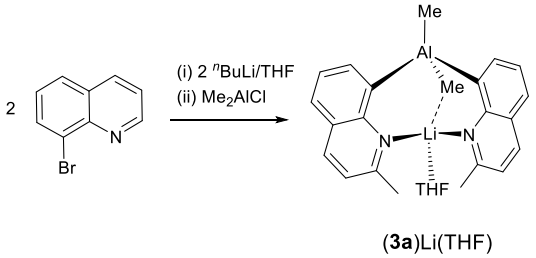

Scheme 3 Synthesis of (**3a**)Li(THF).

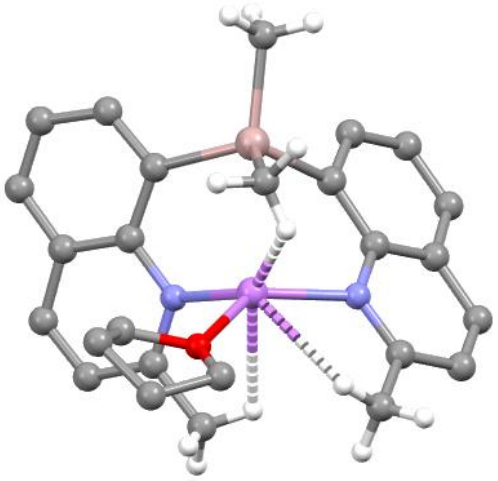

Figure 6 Solid-state structure of [(**3a**)Li(THF)] (in the toluene mono-solvate). H-atoms on the qy groups and the lattice toluene molecule have been omitted for clarity. Selected bond lengths (Å) and angles (°): C_{Me}-Al (terminal) 1.998(2), C_{Me}-Al (bridging) 2.024(3), C_{qy}-Al range 2.019(2)-2.025(3), N-Li range 2.046(5)-2.075(5), C•••Li 2.449(5) (C-H•••Li 1.84), Li-O 2.002(5), Al•••Li 2.808(4), C_{qy}-Al-C_{qy} 109.03(10), N-Li-N 113.6(2), O-Li-N range 97.50(19)-135.3(2), Al-C•••Li 77.1(1). Colour code: C (grey), Al (pink), N (blue), Li (magenta), O (red).

In a background study we also prepared and structurally characterised the 6-methyl-2-pyridyl analogue of **3a** [Me_2Al(6-Me-2-py)$_2$]$^-$ (**4**), which was isolated as the bis-THF adduct [(**4**)Li(THF)$_2$] (see ESI). Not unexpectedly, bis-THF solvation of the Li^+ cation is preferred to the monosolvation and accompanying Al–Me•••Li interaction that is observed for the quinolyl system. It can therefore be concluded that the unusual arrangement in [(**3a**)Li(THF)] arises primarily from the steric effects of the 2-Me-8-qy groups on the coordination site of the aluminate anion, as well as the change in geometry required to accommodate the additional distance between the N-donor atom and the Al bridgehead.

DFT calculations were carried out on [(**3a**)Li(THF)] to explore the nature of the bonding within the Al–Me•••Li bridge. The data presented here were geometry optimised at the TPSS[27]/def2-TVZP[28,29] level of theory, which produced Li–H and Li–C bond lengths that were most consistent with the X-ray structure. However, the results were also confirmed using BP86[30–32] and B3LYP[33,34] functionals. A single point calculation of the optimised structure was used for the population and NBO analyses.[35,36] From these calculations (Figure 7), it can be seen that the formation of the Al–Me•••Li interaction results in weakening of the Al–C bond compared to the terminal Al–C bond and a small net increase in the total negative charge of the Me group (from −1.20e for the terminal CH_3 group to −1.21e for the bridging CH_3, −0.59e to −0.61e for their C atoms). From the Wiberg bond order and second-order perturbation theory, the presence of a very weak interaction largely involving one of the H-atoms and the C-atom of the bridging Me-group can be assumed (see ESI for further details). A σ(C–H)•••Li delocalisation energy of 3.72 kcal mol^{-1} was computed. To verify the nature of this C–H•••Li interaction further and to classify it either as hydrogen bond or agostic interaction, an Atoms in Molecules (AIMS) analysis[37] was carried out (see Figure 7). From

this a bond critical point between the bridging carbon atom and the lithium was identified. The electron density at the bond critical point of the C–Li interaction is −0.402 eV, from which the bond energy for this interaction can be estimated to be 2.55 kcal mol^{-1} (in line with the NBO analysis, with delocalisation energy of 3.72 kcal mol^{-1}).[38] However, no bond critical point could be found between the H and Li atoms using the AIMS approach. Based on the NBO results and the AIMS analysis, the distinction between a weak hydrogen bond or agostic interaction is not trivial and can lead to mis-assigned interactions.[39] However, despite the reduced charge on H, which is typical for agostic interactions, the geometric parameters of the Al–Me•••Li bridge, such as the large Li–H•••C bond angle of 117° and the presence of different Li•••H and Li•••C distances, point more towards the existence of a weak hydrogen bond rather than an agostic interaction.[40] This conclusion is in line with a recent combined experimental and theoretical study that suggested that an NBO based σ(C–H)•••M delocalisation energy of >5.0 kcal mol^{-1} is characteristic of an agostic interaction (i.e., well above the 2.55 kcal mol^{-1} calculated for the interaction in [(**3a**)Li(THF)]).[41]

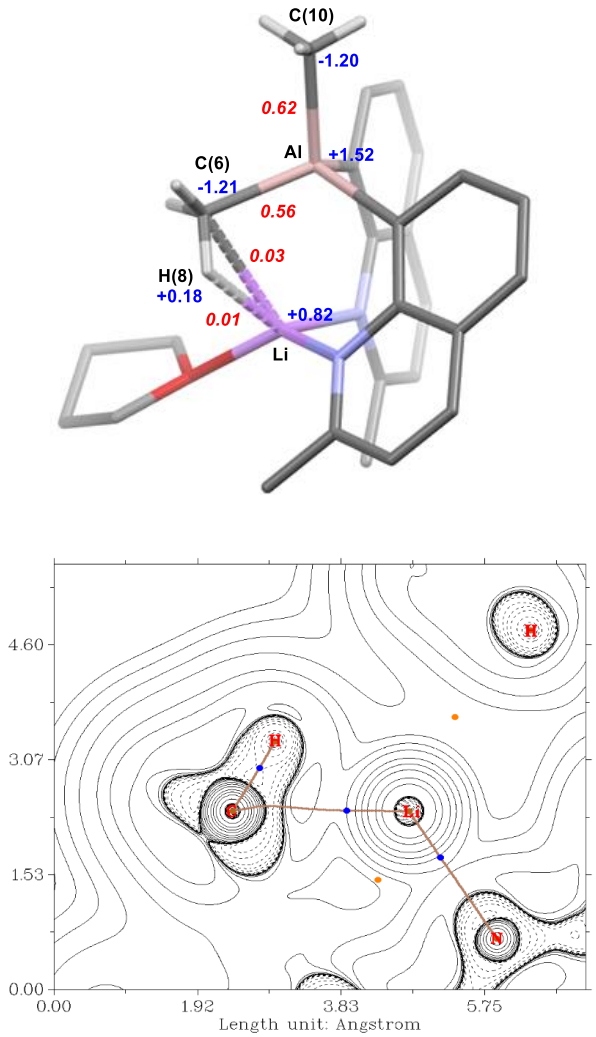

Figure 7 Top: Selected natural charges (in blue) and NBO bond orders (in red) from the TPSS[27]/def2-TVZP[28,29] optimised structure of [(**3a**)Li(THF)]. Bottom: Graph of the Laplacian of the electron density of compound [(**3a**)Li(THF)]. The red lines represent bond critical paths and the blue points are bond critical points within the Li(2)–C(6)–H(8) plane. The numbering scheme refers to that applied in the DFT calculations.

Repeated attempts to prepare the analogue of [(**3a**)Li(THF)] containing an Et_2Al bridgehead, [{Et_2Al(2-Me-8-qy)$_2$}$_2$Li(THF)] [(**3b**)Li(THF)], using the same synthetic procedure but with Et_2AlCl in place of Me_2AlCl, unexpectedly produced the crystalline aluminate complex [{{EtAl(2-Me-8-qy)$_2$}$_2$O}(Li_2THF)] (**5**) in variable yields from a few crystals up to 23% (with respect to Et_2AlCl supplied). The complex contains an [{EtAl(2-Me-8-qy)$_2$}$_2$O]$^{2-}$ dianion in which two Al centres are bridged together by an oxo-ligand. This arrangement notionally results from reaction of the desired product [(**3b**)Li(THF)], with adventitious H_2O during crystallisation at −20 °C or present in the solvent used, supported by the observation of ethane formation as one of the by-products (Scheme 4). However, attempts to obtain the complex by the deliberate addition of a stoichiometric amount of H_2O after in situ formation [(**3a**)Li(THF)] led only to a mixture of products (including free quinoline). Compound **5** proved to be highly moisture sensitive and was characterised only by single-crystal X-ray analysis and elemental analysis. The formation of the complex is of interest with respect to previous studies of the hydrolysis and alcoholysis of lithium tris(2-pyridyl)aluminate complexes, which showed that the Al–C bonds to the 2-pyridyl groups are considerably more reactive than the Al-bonded alkyl groups of the bridgehead;[15,23] the opposite to the reactivity pattern observed for the putative intermediate [(**3b**)Li(THF)]. A potential explanation for this is provided by the previously discussed DFT calculations of [(**3a**)Li(THF)], which showed that bridging of the Me-group between the Al and Li atoms results in significant weakening of the Al–C bond compared to the terminal Me–Al bond (as seen in the reduction in NBO bond order from 0.62 to 0.56).

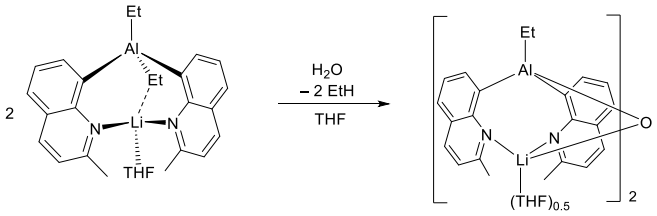

(**3b**)Li(THF) **5**

Scheme 4 The partial hydrolysis of [(**3b**)Li(THF)] with adventitious H_2O.

The molecular structure of **5** consists of an [{EtAl(2-Me-8-qy)$_2$}$_2$O]$^{2-}$ dianion in which two [EtAl(2-Me-8-qy)$_2$] subunits are joined together by a bridging O-atom (Figure 8). There are two chemically distinct Li environments in this arrangement, with both Li^+ cations being coordinated by the two quinolyl N-atoms from each [EtAl(2-Me-8-qy)$_2$] subunit (range 2.088(5)-2.175(5) Å), but with one THF being solvated while in the other the THF solvation is replaced by a long-range μ-N•••Li interaction with a quinolyl N-atom of the other [EtAl(2-Me-8-qy)$_2$] subunit (2.467(5) Å). As a result, both Li^+ cations have distorted tetrahedral geometries.

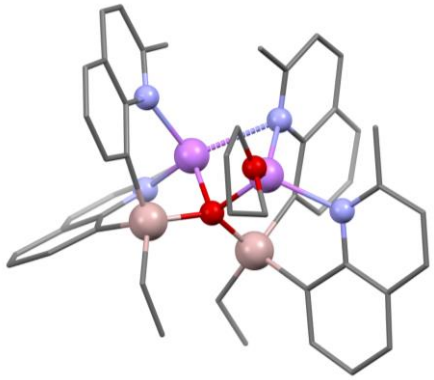

Figure 8 Solid-state structure of **5**. H-atoms and the lattice THF molecule have been omitted for clarity. Selected bond lengths (Å) and angles (°): C_{Et}-Al 1.995(3)-2.003(3), C_{qy}-Al range 2.015(3)-2.042(3), Al-O range 1.7693(17)-1.7720(17), N-Li range 2.088(5)-2.175(5) (the longest of these bonds is to the μ-N-quinolyl group), μ-N_{qy}••Li 2.467(5), Li-O_{oxo} range 1.926(5)-1.947(4), C_{qy}-Al-C_{qy} range 105.10(10)-106.90(10), Al-O-Al 135.47(10), N_{qy}-Li-N_{qy} 100.49(19)-107.0(2) (within each subunit), Li-(μ-N_{qy})•••Li 76.52(16). Colour code: C (grey), Al (pink), N (blue), Li (magenta), O (red).

Conclusion

The results of this investigation show that moving the donor N-atom from the 2-position of 2-pyridyl or 2-quinolyl groups to the more remote position in 8-quinolyl substituents has a large effect on the coordination of Li^+ cations in the corresponding aluminate complexes. This is seen perhaps most dramatically in the structure of [{EtAl(2-Me-8-qy)$_3$}Li] (**2**Li), in which the Li^+ cation has an unusual three-coordinate, trigonal planar arrangement stemming from a combination of steric effects and the geometric constraints of the donor N-atoms. The bis(quinolyl)aluminate complex [{Me_2Al(2-Me-8-qy)$_2$}Li(THF)] [(**3a**)Li(THF)] is of particular interest, in which N-donor bonding in the tris(2-methyl-8-quinolyl)aluminate is replaced by a bridging C–H•••Li interaction. The adventitious reaction of the closely related complex [{Et_2Al(2-Me-8-qy)$_2$}Li(THF)] [(**3b**)Li(THF)] with H_2O gives the O-bridged [{EtAl(2-Me-8-qy)$_2$}$_2$O]$^{2-}$ dianion. Interestingly, this reactivity is the opposite of that seen in the case of tris(2-pyridyl)aluminates [RAl(2-py)$_3$]$^-$, in which the 2-py groups are more basic than the R-group. Overall, the results illustrate that functionalisation of the aluminate frameworks with polyaromatic N-donor substituents provides the means of introducing radically different coordination environments and that this should be a promising area of study in the future.

Experimental Section

General Experimental Methods

Syntheses were carried out on a Schlenk line under a nitrogen atmosphere using oven-dried glassware, unless otherwise specified. Starting materials were commercially obtained from suppliers and used as received. Lower temperatures in synthesis were achieved using dry ice/acetone (−78 °C) baths. MeCN and CH_2Cl_2 were dried over CaH_2 and distilled under nitrogen. Et_2O, *n*-hexanes and THF were dried over Na/benzophenone and distilled under nitrogen. Deuterated solvents were distilled and/or dried over molecular sieves before use. A nitrogen-filled glove box (Saffron type α) was used to manipulate solids, including room temperature reactions, product recovery and sample preparation for analysis. Yields are given as isolated yields of solid or crystalline products. Room temperature ^{1}H, ^{7}Li, ^{13}C{^{1}H} and ^{27}Al NMR spectra were recorded on a Bruker 400 MHz Avance III HD Smart Probe spectrometer and referenced to the residual solvent peaks. For ^{27}Al and ^{7}Li NMR, external references were used ($AlCl_3$·$6H_2O$ and 1 M LiCl in D_2O, respectively). Unambiguous assignments of NMR resonances were made on the basis of 2D NMR experiments (^{1}H-^{1}H COSY, ^{1}H-^{13}C HSQC and ^{1}H-^{13}C HMBC). Figure 9 shows the labelling scheme for NMR assignments. Mass spectra were obtained by positive ion electrospray ionisation using a Thermo Fisher Orbitrap mass spectrometer. Elemental analysis for carbon, hydrogen, and nitrogen was performed using a Perkin Elmer 240 Elemental Analyser. X-ray crystallographic data were collected using either a Nonius KappaCCD (sealed-tube MoKa) or a Bruker D8-QUEST PHOTON-100 (Incoatec IμS Cu microsource) diffractometer. The temperature was held at 180(2) K using an Oxford Cryosystems N_2 cryostat. Structures were solved using SHELXT[42] and refined using SHELXL.[43]

Synthesis of New Compounds

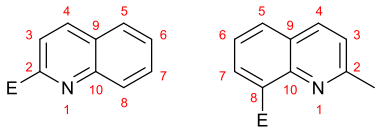

Figure 9. Labelling scheme for NMR assignments.

[{EtAl(2-qy)$_3$}Li(μ-X)Li(THF)$_3$] (X = Cl/Br 62:38) [(1)Li(μ-X)Li(THF)$_3$] and [{(EtAl(2-qy)$_3$)Li}$_2$(μ-Br)]$^-$Li(THF)$_4^+$ [{1Li}$_2$(μ-Br)]$^-$Li(THF)$_4^+$: A solution of 2-bromoquinoline (900 mg, 4.32 mmol) in THF (30 mL) was cooled to −78 °C. ^{n}BuLi (1.6 M in hexanes, 2.7 mL, 4.32 mmol) was added dropwise and the red solution was stirred at −78 °C for 2.5 h. In a separate flask, ethylaluminium dichloride (1.0 M in hexanes, 1.43 mL, 1.43 mmol) was diluted in 10 mL THF and kept at −78 °C. This solution was transferred to the first flask (containing 2-lithio-quinoline) dropwise with a cannula. The solution was allowed to warm to room temperature and stirred overnight. The volatiles were removed from the dark brown solution under vacuum, and toluene (20 mL) and THF (5 mL) were added to the residue. The mixture was gently heated, filtered, and concentrated under vacuum. Storage at −15 °C afforded a few colourless crystals which were shown to be a mixture of both products by X-ray crystallography. ^{1}H NMR (298 K, D_8-THF, 400 MHz), δ [ppm] = 8.79 (d, 3 H, H8, J_{HH} 8.4), 7.89 (d, 3 H, H3, J_{HH} 8.1), 7.82 (d, 3 H, H4, J_{HH} 8.1), 7.65 (d, 3 H, H5, J_{HH} 7.7), 7.56-7.52 (m, 3 H, H6/H7), 7.32 (dd, 3 H, H6/H7, J_{HH} 7.6), 1.56 (t, 3 H, Et-CH_3, J_{HH} 7.2), 0.78 (q, 2 H, Et-CH_2, J_{HH} 8.1). ^{13}C{^{1}H} NMR (298 K, D_8-THF, 126 MHz): δ [ppm] = 194.4 (br, C2, detected through ^{1}H-^{13}C HMBC experiment), 151.2 (C6 or C5), 149.8 (C5 or C6), 131.0 (C3), 130.9 (C4), 129.7 (C7), 128.6 (C10), 128.1 (C8), 124.9 (C9), 11.21

(Et-CH_3), −0.2 (br, Et-CH_2, detected through ^{1}H-^{13}C HMQC). ^{27}Al NMR (298 K, D_8-THF, 130 MHz): δ [ppm] = 128 (br, s). ^{7}Li NMR (298 K, D_8-THF, 194 MHz): δ [ppm] = 1.02.

[{EtAl(2-Me-8-qy)$_3$}Li] [(2)Li]: A solution of 2-bromoquinoline (666 mg, 3.00 mmol) in THF (40 mL) was cooled to −78 °C. ^{n}BuLi (1.6 M in hexanes, 1.9 mL, 3.00 mmol) was added dropwise and the red solution was stirred at −78 °C for 1 h. Ethylaluminium dichloride (0.9 M in heptane, 1.5 mL, 1.5 mmol) was added. The solution was allowed to warm to room temperature and stirred overnight. The volatiles were removed from the orange solution under vacuum. The residue was extracted with toluene (40 mL) and filtered through Celite. The solution was concentrated under vacuum until a precipitate formed. The precipitate was dissolved by the addition of THF (ca. 5 mL), and the solution was stored in the freezer at −20 °C. Needle-like colourless crystals were collected by filtration and dried under vacuum. Isolated yield (two batches) 416 mg (0.850 mmol, 43%).^{1}H NMR (298 K, CD_2Cl_2, 400 MHz), δ [ppm] = 8.22 (dd, 3 H, H7, J_{HH} 6.7, 1.4), 8.11 (d, 3 H, H4, J_{HH} 8.3), 7.63 (dd, 3 H, H5, J_{HH} 8.0, 1.4), 7.42 (dd, 3 H, H6, J_{HH} 7.8, 6.7), 7.16 (d, 3 H, H3, J_{HH} 8.3), 2.18 (s, 9 H, qy-CH_3), 1.40 (t, 3 H, Et-CH_3, J_{HH} 7.9), 0.72 (q, 2 H, Et-CH_2, J_{HH} 7.9). ^{13}C{^{1}H} NMR (298 K, CD_2Cl_2, 101 MHz), δ [ppm] = 156.5 (C2), 154.7 (C10), 142.2 (C7), 139.6 (C4), 126.4 (C9), 126.3 (C6), 126.2 (C5), 120.8 (C3), 24.3 (qy-CH_3), 11.4 (Et-CH_3). C8 and Et-CH_2 not observed. ^{27}Al NMR (298 K, CD_2Cl_2, 104 MHz), δ [ppm] = 137.2. ^{7}Li NMR (298 K, CD_2Cl_2, 155 MHz), δ [ppm] = 4.9. Elemental analysis (%): calcd for $C_{32}H_{29}AlLiN_3$ C 78.5, H 6.0, N 8.6; found C 77.6, H 5.8, N 8.6.

[{Me$_2$Al(2-Me-8-qy)$_2$}Li(THF)] [(3a)Li(THF)]: A solution of 8-bromo-2-methylquinoline (666 mg, 3.00 mmol) in THF (40 mL) was cooled to −78 °C. ^{n}BuLi (1.6 M in hexanes, 1.9 mL, 3.00 mmol) was added dropwise and the red solution was stirred at −78 °C for 1 h. Dimethylaluminium chloride (1.0 M in hexanes, 1.5 mL, 1.5 mmol) was added. The solution was allowed to warm to room temperature and stirred overnight. The volatiles were removed from the orange solution under vacuum. The residue was extracted with toluene (40 mL) and filtered through Celite. The solution was concentrated under vacuum until a precipitate formed. The precipitate was dissolved by the addition of THF (ca. 5mL), and the solution was stored in the freezer at −20 °C. Needle-like colourless crystals were collected by filtration and dried under vacuum. Isolated yield (two batches) 320 mg (0.762 mmol, 50%). ^{1}H NMR (298 K, D_8-THF, 400 MHz), δ [ppm] = 8.25 (dd, 2 H, H7, J_{HH} 6.7, 1.1), 8.06 (d, 2 H, H4, J_{HH} 8.2), 7.56 (dd, 2 H, H5, J_{HH} 8.1, 1.4), 7.42 (dd, 2 H, H6, J_{HH} 8.1, 7.5) 7.17 (d, 2 H, H3, J_{HH} 8.3), 2.70 (s, 6 H, qy-CH_3), −0.34 (s, 6 H, Al-CH_3) (the THF ligand is partially or completely absent as a result of the lability of the ligand in the complex when placed under vacuum during isolation). ^{13}C{^{1}H} NMR (298 K, D8-THF, 101 MHz), δ [ppm] = 155.9 (C2), 154.6 (C9), 140.8 (C7), 138.7 (C4), 125.9 (C10), 125.3 (C6), 124.8 (C5), 120.0 (C3), 24.0 (qy-CH_3). C8 and Al-CH_3 not observed. ^{27}Al NMR (298 K, D_8-THF, 104 MHz), δ [ppm] = 146.9. ^{7}Li NMR (298 K, D_8-THF, 155 MHz), δ [ppm] = 3.5. Elemental analysis (%): calcd for $C_{22}H_{22}AlLiN_2$ (THF molecule removed) C 75.8, H 6.4, N 8.0; found C 75.5, H 6.9, N 8.3.

[{{EtAl(2-Me-8-qy)$_2$}$_2$O}(Li$_2$THF)] (5): A solution of 8-bromo-2-methylquinoline (666 mg, 3.00 mmol) in THF (40 mL) was cooled to −78 °C. ^{n}BuLi (1.6 M in hexanes, 1.9 mL, 3.00 mmol) was added dropwise and the red solution was stirred at −78 °C for 1 h. Diethylaluminium chloride (1.0 M in hexanes, 1.5 mL, 1.5 mmol) was added. The solution was allowed to warm to room temperature and stirred overnight. The volatiles were removed from the orange solution under vacuum. The residue was extracted with toluene (40 mL) and filtered through Celite. The solution was concentrated under vacuum until a precipitate formed. The precipitate was dissolved by the addition of THF (ca. 5 mL), and the solution was stored in the freezer at −20 °C. Needle-like colourless crystals were collected by filtration and dried under vacuum. Isolated yield (first reaction) 0.246 mg (0.346 mmol, 23%), however, further attempts produced variable yields lower than this. Elemental analysis (%): calcd for $C_{44}H_{42}Al_2Li_2N_4O$ C 74.3, H 6.0, N 7.9; found C 73.8, H 5.9, N 7.6.

Acknowledgements

We thank the Walters-Kundert Studentship of Selwyn College (scholarship for J.E.W.), the Leverhulme Trust (R.G.-R. and D.S.W.), the Australian Research Council (A.L.C., DE200100450), the Young Investigator Group preparation program at KIT funded by the Federal Ministry of Education and Research (BMBF) and the Baden-Württemberg Ministry of Science as part of the Excellence Strategy of the German Federal and State Governments. (S.H.), the state of Baden-Württemberg through bwHPC and the German Research Foundation (DFG) through grant no INST 40/575-1 FUGG (JUSTUS 2 cluster) (S.H.), and the Spanish MINECO-AEI and The EU (ESF) for a Ramon y Cajal contract (R.G.-R., RYC-2015-19035).

Author Contributions

J.E.W., A.L.C. and M.R.-N. performed the synthetic studies. S.H. did the DFT calculations. A.D.B. collected and solved crystal data. D.S.W., A.L.C. and R.G.-R. supervised the studies. D.S.W. and A.L.C. wrote the paper.

Conflicts of interest

The authors declare that there are no conflicts of interest.

Keywords: quinolyl • aluminate • main group synthesis • ligands

1 L. Gade, P. Hoffman, *Molecular Catalysts: Structure and Functional Design*, Wiley-VCH, **2014**.
2 C. Moberg, *Angew Chem. Int. Ed*. 1998, **7**, 248-268.
3 N. L. Lampland, M. Hovey, D. Mukherjee, A. D. Sadow, *ACS Catal*. 2015, **5**, 4219-4226.
4 A. G. Walden, A. J. M. Miller, *Chem Sci*. 2015, **6**, 2405-2410.
5 S. E. Gibson, M. P. Castaldi, *Chem. Commun*. 2006, 3045; P. Etayo, C. Ayats, M. A. Pericàs *Chem. Commun*. 2016, **52**, 1997.
6 S. Trofimenko, *Chem Rev*. 1972, **72**, 497-509.
7 S. Trofimenko, S. J. Lippard, ed. *Progress in Inorganic Chemistry*. John Wiley & Sons, Ltd; 1986.

8 S. Trofimenko S. *Recent Advances in Poly(Pyrazolyl)Borate (Scorpionate) Chemistry*. Vol 93, 1993.
9 J. F. Ojo, P. A. Slavin, J. Reglinski, M. Garner, M. D. Spicer, A. R. Kennedy, S. J. Teat., *Inorg. Chim Acta*. 2001, **313**, 15-20.
10 L. F. Szczepura, L. M. Witham, K. J. Takeuchi, *Coord Chem Rev*. 1998, **174**, 5-32.
11 For example, C. S. Alvarez, F. García, S. M. Humphrey, A. D. Hopkins, R. A. Kowenicki, R. A. Layfield, M. McPartlin, R. Raja, M. C. Rogers, A. D. Woods and D. S. Wright, *Chem. Commun.* 2005, 198-200.
12 H. R. Simmonds, D. S. Wright, *Chem Commun*. 2012, 48, 8617-8624; A. J. Peel, A. J. Plajer, J. E. Waters, R. García-Rodríguez, D. S. Wright, *Adv. Organomet. Chem.* 2021, **75**, 193-244.
13 A. J. Plajer, A. L. Colebatch, F. J. Rizzuto, P. Pröhm, A. D. Bond, R. Garcia-Rodriguez, D. S. Wright, *Angew. Chem. Int. Ed*. 2018, **57**, 6648-6652.
14 R. García-Rodríguez, S. Kopf, D. S. Wright, *Dalton Trans*. 2018, **47**, 2232-2239.
15 R. García-Rodríguez, S. Hanf, A. D, Bond, D. S. Wright, *Chem. Commun*. 2017, **53**, 1225-1228.
16 G. M. Pawar, J. B. Sheridan, F. Jäkle, *Eur. J. Inorg. Chem*. 2016, 2227-2235.
17 (a) M. S. Deshmukh, A. Yadav, R. Pant, R. Boomishankar, *Inorg Chem*. 2015, 54, 1337-1345; (b) M. S. Deshmukh, V. S. Mane, A. S. Kumbhar, R. Boomishankar, *Inorg. Chem.* 2017, **56**, 13286-13292.
18 E. S. Yang, A. J. Plajer, A., García-Romero, A. D. Bond, T. K. Ronson, C. M. Álvarez, R. García-Rodríguez, A. L. Colebatch, D. S. Wright, *Chem. Eur. J.* 2019, **25**, 14003.
19 N. Wei, N. N. Murthy, K. D. Karlin, *Inorg Chem*. 1994;33, 6093-6100.
20 T. H. Bullock, W. T. K. Chan, D. J. Eisler, M. Streib, D. S. Wright, *Dalton Trans*. 2009, 1046-1054.
21 T. H. Bullock, W. T. K. Chan, D. S. Wright, *Dalton Trans*. 2009, 6709-6711.
22 R. García-Rodríguez, T. H. Bullock, M. McPartlin, D. S. Wright, *Dalton Trans*. 2014, **43**, 14045-14053.
23 R. García-Rodríguez, D. S. Wright, *Chem. Eur. J.* 2015, **21**, 14949-14957.
24 Search of the Cambridge Crystallographic Data Base (May 2021) on lithium aluminates. For the search, the range of the Al-C-H•••Li contacts was restricted to 1.80-2.20 Å (in line with D. Braga, F. Grepioni, K. Brasha, G. R. Desiraju, *Dalton Trans*. 1996, 3925).
25 See also, J. M. Cole, P. G. Waddell, A. E. H. Wheatley, G. J. McIntyre, A. J. Peel, C. W. Tate, D. J. Linton, *Organometallics* 2014, **33**, 3919-3923; J. O. Bauer, C. Strohman, *Organometallics* 2021, **40**, 11-15.
26 (a) K. Zechert, D. Fuhrmann, *Inorg. Chem.* 2019, **58**, 16736-16742; (b) K. Zechert, *Oranometallics*, 2013, **32**, 1387-1393.
27 J. Tao, J.P. Perdew, V. N. Staroverov, G. E. Scuseria, *Phys. Rev. Lett.* 2003, **91**, 146401-146404.
28 F. Weigend, *Phys. Chem. Chem. Phys.* 2006, **8**, 1057–1065.
29 F. Weigend, R. Ahlrichs, *Phys. Chem. Chem. Phys.* 2005, **7**, 3297–3305.
30 A. D. Becke, *Phys. Rev. A* 1988, **38**, 3098–3100.
31 J. P. Perdew, *Phys. Rev. B* 1986, **33**, 8822–8824.
32 J. P. Perdew, *Phys. Rev. B* 1986, **34**, 7406.
33 A. D. Becke, *J. Chem. Phys.* 1993, **98**, 5648–5652.
34 P. J. Stephens, F. J. Devlin, C. F. Chabalowski, M. J. Frisch, *J. Phys. Chem.* 1994, **98**, 11623–11627.
35 E. D. Glendening, A. E. Reed, J. E. Carpenter, F. Weinhold, NBO Version 3.1. (1998).
36 Reed, A. E., Curtiss, L. A. & Weinhold, F. NBO. *Chem. Rev.* 1988, **88**, 899–926.
37 Atoms in Molecules - R. F. W. Bader - Oxford University Press. https://global.oup.com/academic/product/atoms-in-molecules-9780198558651?cc=de&lang=en&.
38 S. Emamian, T. Lu, H. Kruse, H. Emamian, H. *J. Comput. Chem.* 2019, **40**, 2868–2881.
39 T. S. Thakur, G. R. Desiraju, *Chem. Commun.* 2006, 552–554.
40 D. Braga, F. Grepioni, E. Tedesco, K. Biradha, G. R. Desiraju, *Organometallics* 1997, **16**, 1846.
41 T. S. Thakur, G. R. Desiraju, *J. Mol. Struct. THEOCHEM* 2007, **810**, 143–154.
42 G. M. Sheldrick, *Acta Cryst. A* 2015, **71**, 3-8.
43 G. M. Sheldrick, *Acta Cryst. C* 2015, **71**, 3-8.

Entry for the Table of Contents

Synthesis and Coordination Behaviour of Aluminate-based Quinolyl Ligands

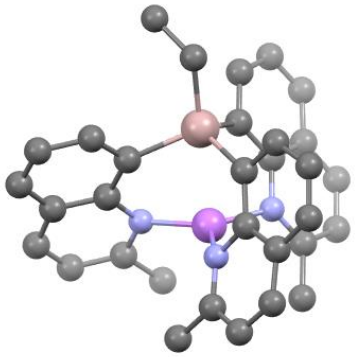

J. E. Waters, S. Hanf, M. Rincón-Nocito, A. D. Bond, R. García-Rodríguez, D. S. Wright,* A. L. Colebatch*

The effects of moving the donor N-atom from the 2-position in lithium (2-pyridyl)aluminates to the more remote position in (8-quinolyl)aluminates have been investigated by solid-state structural and DFT calculations, with large differences in the coordination of the Li^+ cations by the aluminate anions being found.